The Hoiamides, Structurally Intriguing Neurotoxic Lipopeptides from Papua New Guinea Marine Cyanobacteria

Hyukjae Choi,[†] Alban R. Pereira,[†] Zhengyu Cao,[‡] Cynthia F. Shuman,[†] Niclas Engene,[†] Tara Byrum,[†] Teatulohi Matainaho,[§] Thomas F. Murray,[‡] Alfonso Mangoni,*[,⊥] and William H. Gerwick*[,†]

Center for Marine Biotechnology and Biomedicine, Scripps Institution of Oceanography, and Skaggs School of Pharmacy and Pharmaceutical Sciences, University of California, San Diego, La Jolla, California 92093, Discipline of Pharmacology, School of Medicine and Health Sciences, University of Papua New Guinea, National Capital District, Papua New Guinea, Department of Pharmacology, School of Medicine, Creighton University, Omaha, Nebraska 68178, and Dipartimento di Chimica delle Sostanze Naturali, Università di Napoli "Federico II", Via D. Montesano 49, 80131 Napoli, Italy

Received July 8, 2010

Two related peptide metabolites, one a cyclic depsipeptide, hoiamide B (**2**), and the other a linear lipopeptide, hoiamide C (**3**), were isolated from two different collections of marine cyanobacteria obtained in Papua New Guinea. Their structures were elucidated by combining various techniques in spectroscopy, chromatography, and synthetic chemistry. Both metabolites belong to the unique hoiamide structural class, characterized by possessing an acetate extended and *S*-adenosyl methionine modified isoleucine unit, a central triheterocyclic system comprised of two α-methylated thiazolines and one thiazole, and a highly oxygenated and methylated C-15 polyketide unit. In neocortical neurons, the cyclic depsipeptide **2** stimulated sodium influx and suppressed spontaneous Ca^{2+} oscillations with EC_{50} values of 3.9 μM and 79.8 nM, respectively, while **3** had no significant effects in these assays.

Cyanobacteria are well recognized to be rich producers of structurally intriguing and biologically active secondary metabolites, many of which have toxic properties.[1] Indeed, freshwater cyanobacteria have been studied since the 1930s because their toxins have impacted both human populations and domestic animals.[2] On the other hand, marine cyanobacteria have been highlighted in the natural products chemistry field because their metabolites have interesting structures and pharmacology and are thus of high potential pharmaceutical utility. Recognition of this fact began more than 30 years ago with the discovery of majusculamides A and B by R. E. Moore in 1977.[3] To date, more than 700 secondary metabolites have been reported with various biological properties including inhibition of microtubules (curacin A),[4a,b] inhibition of angiogenesis and promotion of actin polymerization (hectochlorin),[4c] sodium channel blocking (kalkitoxin)[4d] and activating activities (antillatoxin),[4e] and G1 cell cycle arrest and induction of apoptosis (apratoxin A).[4f,g] Biosynthetically, marine cyanobacteria produce secondary metabolites of a variety of structure classes, including peptides, polyketides, terpenoids, and alkaloids. However, the most predominant structure class are lipopeptides, which are formed by the integration of polyketide synthases (PKS) and nonribosomal peptide synthetases (NRPS).[5] More than 36% of the known cyanobacterial secondary metabolites are formed from polyketides transitioning into nonribosomal peptides, an orientation termed "ketopeptides" (251 compounds), and 9% are peptides transitioning into polyketides, known as "peptoketides" (63 compounds).[1] Slightly more than 30% of the ketopeptides and peptoketides are a complex mixture of these nonribosomal peptide and polyketide components. In addition, cyanobacterial lipopeptides are highly modified by various biosynthetic enzymes in their complicated biosynthetic pathways, including by halogenations, unusual oxidations, and a variety of *C*-, *O*-, and *N*-methylations. In some cases, the complex biosynthetic origin and extensive secondary modification of cyanobacterial lipopeptides make their structural elucidation challenging.

The voltage-gated sodium channel (VGSC) is an important drug target and is the site of action for several classes of pharmaceutical agents, including local anesthetics (bupivacaine, cocaine, and lidocaine), antiarrhythmics (flecainide and propafenone), anticonvulsants (carbamazepine, phenytoin, and valproic acid), and analgesics (ziconotide); new treatments for neurodegenerative disorders are also being developed for this target.[6] The VGSC allows passage of Na^+ across membranes and thus plays an important role in the generation of action potentials in excitable cells such as neurons.[7a] In the open state, the pore of the VGSC is open and allows Na^+ influx into the cytoplasm of the cell, which then produces a regenerative membrane depolarization. The VGSC complex consists of a large α-subunit, critical for channel pore formation and voltage sensing, and one or two auxiliary α-subunits.[7a−c] VGSCs represent the molecular targets for toxins that act at six or more distinct neurotoxin sites on the channel protein.[7d] Tetrodotoxin, saxitoxin, and δ-conotoxins GIIIA and GIIIB, binding to neurotoxin site 1, block the channel pore and inhibit sodium flux. Batrachotoxin and veratridine, acting on neurotoxin site 2, inhibit VGSC inactivation. α-Scorpion, δ-conotoxin, and the sea anemone toxins, targeting neurotoxin site 3, also retard inactivation of the VGSC, whereas β-scorpion toxins, interacting with neurotoxin site 4, shift the voltage dependence of activation to more negative membrane potentials without an effect on channel inactivation. Brevetoxins and ciguatoxins link to neurotoxin site 5 and stimulate channel activity by shifting the activation potential to more negative values and blocking channel inactivation. δ-Conotoxin interacting with neurotoxin site 6 delays channel inactivation. Pyrethroids and DDT are coupled to neurotoxin site 7 and produce effects similar to site 5 toxins.

Recently, we reported a cyclic depsipeptide named hoiamide A (**1**), which illustrates a new chemotype within the natural products of cyanobacteria and possesses potent neuropharmacological properties.[8] It was found that compound **1** inhibits the binding of [^{3}H]batrachotoxin to site 2 of the mammalian VGSC and stimulates sodium influx in neocortical neurons as a partial agonist. Structurally, it possesses a stereochemically complex structure (15 chiral centers) with highly modified peptide and polyketide units as well as an unusual triheterocyclic section.

* To whom correspondence should be addressed. Tel: (858) 534-0578. Fax: (858) 534-0529. E-mail: wgerwick@ucsd.edu; alfonso.mangoni@unina.it.

[†] University of California, San Diego.

[‡] Creighton University.

[§] University of Papua New Guinea.

[⊥] Università di Napoli "Federico II".

10.1021/np100468n
Published on Web 08/05/2010

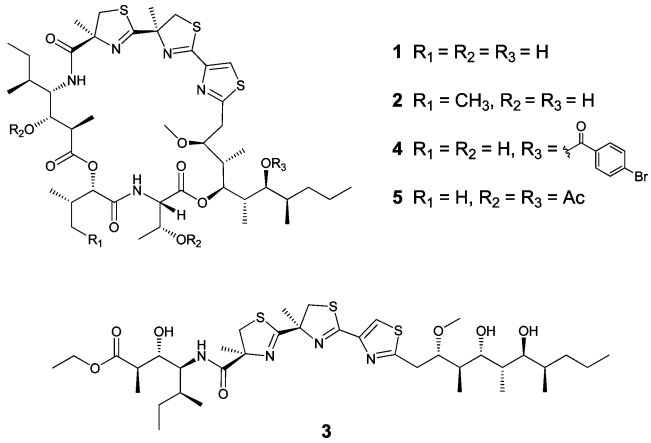

Figure 1. Structures of natural hoiamides A−C (**1**−**3**) and hoiamide A analogues **4**[8] and **5**.[8]

As part of an ongoing neuropharmacological screening program aimed at discovering additional neurotoxins produced by marine organisms, we investigated the extracts of two independent collections of Papua New Guinea marine cyanobacteria. The first extract, prepared from an assemblage of *Symploca* sp. and *Oscillatoria cf.* sp., exhibited potent inhibition of calcium oscillation and activation of sodium influx in mouse neocortical neurons. ^{1}H NMR-guided fractionation of this material afforded the new cyclic depsipeptide hoiamide B (**2**), along with the known metabolite hoiamide A (**1**). The second extract, derived from a *Symploca* sp. specimen, showed mild brine shrimp toxicity, and its fractionation led to the discovery of the linear hoiamide C (**3**). Herein, we report the isolation, structure elucidation, and biological activity of hoiamides B (**2**) and C (**3**) as the newest members of this unique structural class, the hoiamides.

Results and Discussion

Isolation and Structure Elucidation of Hoiamide B (2). A collection of tuft-forming marine cyanobacteria was obtained via scuba at Gallows Reef, Papua New Guinea, in 2006 (PNG-4-28-06-1). The collection was extracted repeatedly with CH_2Cl_2−MeOH (2:1) and further fractionated by silica gel vacuum column chromatography (VLC) to produce nine fractions (A−I). The F fraction was found to possess potent sodium channel activating activity in neuro-2a cells and inhibited calcium oscillations in mouse cerebrocortical neurons. This fraction was thus subjected to RP HPLC to afford hoiamide B (**2**, 8.9 mg, 1.2%) as well as the previously reported hoiamide A (**1**, 25 mg, 3.4%) (Figure 1).[8]

Hoiamide B (**2**) was obtained as a pale yellow oil, and its LRESIMS showed a molecular ion cluster at *m/z* 962.6/963.6/964.5/965.5/966.4 in a ratio of 100:50:29:10:4, indicating the likely presence of three sulfur atoms in the molecule, as found for hoiamide A (**1**). The molecular formula of **2** was determined as $C_{45}H_{73}N_5O_{10}S_3$ by interpretation of HRESITOFMS data ($[M + H]^+$ *m/z* 940.4584). The IR spectrum of **2** displayed absorption bands at 3375, 1738, and 1604 cm^{-1}, indicating the presence of hydroxy, ester, and amide functionalities, respectively. The ^{1}H and ^{13}C NMR spectrum of **2** in DMSO-d_6 showed peptide and oxygenated polyketide features and included seven downfield-shifted carbons without attached protons (δ_C 176.2, 174.4, 173.3, 170.3, 169.8, 165.8, and 161.7), five exchangeable protons (δ_H 7.84, 6.83, 5.15, 4.92, and 3.97), eight *N*- or *O*-substituted methines (δ_H 5.18, 4.94, 4.51, 4.24, 3.79, 3.77, 3.52, and 3.18), three methyl triplets (δ_H 0.835, 0.831, and 0.70), seven methyl doublets (δ_H 1.15, 0.92, 0.87, 0.86, 0.84, 0.82, and 0.73), and three methyl singlets including one methoxy group (δ_H 3.22, 1.61, and 1.55), as shown in Table 1.

The analysis of 1D and 2D NMR data, including COSY, TOCSY, HSQC, and HMBC, allowed the construction of partial structures A−F, and extensive HMBC analysis provided connections between these six partial structures to afford the planar structure of hoiamide B (**2**) (Figure 2). The first two peptidic fragments, A and B, were found to be threonine (Thr) and 2-hydroxy-3-methylpentanoic acid (Hmpa) by COSY and HMBC spectra analysis. Similarly, two additional spin systems could be constructed, one composed of a methyl doublet (H-19, δ_H 0.84), two methines (H-12, δ_H 2.32; H-13, δ_H 3.77), and a hydroxy proton (OH-13, δ_H 2.32), and the other composed of a methyl doublet (H-18, δ_H 0.92), a methyl triplet (H-17, δ_H 0.83), two methine protons (H-14, δ_H 3.52; H-15, δ_H 1.56), one pair of methylene protons (H-16a, δ_H 1.42; H-16b, δ_H 1.05), and one exchangeable proton from an amide (14-NH, δ_H 6.83). The HMBC correlations from H-13 to C-14 and from NH-14 to C-13 allowed the combination of fragments C and D into a new partial structure comprising 4-amino-3-hydroxy-2,5-dimethylheptanoic acid (Ahdhe). A fifth fragment (E) was revealed as possessing three consecutive heterocyclic rings. The ^{1}H and ^{13}C NMR chemical shifts of C-22 (δ_H 3.82/3.15; δ_C 41.1) and C-26 (δ_H 3.52/3.43; δ_C 42.8) were at shifts consistent with placement of heteroatoms at these two positions. HMBC correlations from H-22a/H-22b/H-23 to C-20/C-21, from H-26a/H-26b/H-27 to C-24/C-25, and from H-30 to C-28/C-29/C-31 allowed assignments of two α-methylated thiazolines and one thiazole. The additional HMBC correlations from H-22a/H-22b to C-24 and from H26a/H26b to C-28 identified that the three heterocyclic rings were successively connected to one another. The final partial structure of compound **2** was elucidated as a 5,7-dihydroxy-3-methoxy-4,6,8-trimethylundecanoyl-derived residue (Dmetua). The methoxy group was placed at C-33 (δ_C 79.3) by an HMBC correlation from H-45 (δ_H 3.24) to C-33. COSY correlations helped to assign the terminal chain of four carbons (C-32/C-33/C-34/C-35) with a methyl branch (C-44) at C-34. A second section of partial structure F, assigned by the COSY and HMBC correlations, was composed of a seven-carbon chain (C-43/C-36/C-37/C-38/C-39/C-40/C-41) with hydroxy (C-37) and methyl branches (C-38). These two sections were linked into partial structure F on the basis of HMBC correlations from H-35 to C-36/C-37 and from H-43 to C-35. Finally, the HMBC correlations from NH-2 to C-5, from H-6 to C-11, from NH-14 to C-20, from H-30 to C-31, from H-32/H-33 to C31, and from H-35 to C-1 allowed connection of these six partial structures, thereby forming the planar structure of hoiamide B (**2**) (Figure 2).

The absolute configuration of the 16 chiral centers in hoiamide B (**2**) was assigned by various means, including degradation reactions to yield chiral fragments followed by chromatographic analysis and additional NMR spectroscopic analyses. The absolute configuration of the Thr residue was assigned as L by acid hydrolysis, derivatization with L-FDLA, and LC-ESIMS analysis. The absolute configuration of the Hmpa residue was determined as 2*S*, 3*S* by comparing the retention time of Hmpa released by acid hydrolysis of **2** with the four synthetic stereoisomers of Hmpa by chiral HPLC.[9] In order to assign the absolute configuration of the modified cysteic acids, **2** was subjected to ozonolysis, oxidative workup, and acid hydrolysis to yield 2-methylcysteic acid (MeCysA). The reaction products were then analyzed by chiral HPLC and compared with the retention times of synthetic 2*S*-MeCysA and 2*R*-MeCysA standards; only 2*S*-MeCysA was detected by this analysis. Therefore, the absolute configuration of C-21 and C-25 was assigned as *S* and *R*, respectively.

The relative configuration of the Ahdhe (C-11−C-20) and Dmetua (C-31−C-45) units was revealed by *J*-based configurational analysis (Figure 3). Homonuclear coupling constants were measured from ^{1}H NMR and 1D-TOCSY spectra, whereas heteronuclear coupling constants were measured using a combination of the HETLOC and HSQMBC experiments. The large coupling constant between H-12 and H-13 ($^3J_{H\text{-}12,\ H\text{-}13}$ = 7.9 Hz) indicated an *anti* relationship between these protons, and the ROESY correlations

Table 1. NMR Spectroscopic Data for Hoiamide B (**2**) in DMSO-d_6 at 600 MHz (^{1}H) and 150 MHz (^{13}C)

residue	position	δ_C	δ_H mult (*J* in Hz)	COSY	HMBC[a]	ROESY
Thr	1	170.3				
	2	58.5	4.51 dd (7.7, 2.8)	NH, 3	1, 3	4, 8
			NH, 7.84 d (7.7)	2	3, 5	4, 6, 7, 10
	3	66.3	4.24 m	2, 4, OH	1, 2, 4	8, 37, 43, 3-OH
			OH, 4.92 d (5.6)	3		
	4	20.2	1.15 d (6.3)	3	2, 3	2, 37
Hmpa	5	169.8				
	6	76.3	4.94 d (3.5)	7	5, 11	8a, 8b, 9, 10, 2-NH
	7	36.4	1.91 m	6, 8, 10	5	9
	8a	22.5	1.28 m	7, 8b		6
	8b		1.09 m	7, 8a		2, 3
	9	11.5	0.70 t (7.4)		7, 8	7
	10	14.9	0.87 d (7.6)	7	6	
Ahdhe	11	174.4				
	12	44.4	2.32 m	13, 19	11, 13, 14	14, 13-OH, 14-NH
	13	71.1	3.77 m	12, OH	11, 12, 14	15, 18, 19
			OH, 5.15 d (4.6)	13	12, 13, 14	12, 13, 14, 15, 16, 17, 14-NH
	14	52.7	3.52 dd (10.2, 6.9)	NH, 15	20	12, 18, 19
			NH, 6.83 d (9.6)	14	13, 14, 20	12, 14, 15, 23, 27, 13-OH
	15	35.7	1.56 m	14, 16a, 16b, 19	14,	13, 13-OH, 14-NH
	16a	25.2	1.42 m	15, 16b, 17	17	
	16b		1.05 m	16a, 17	14, 15, 17, 18	
	17	10.6	0.834 t (7.0)	16		
	18	13.7	0.92 d (6.9)	15	14, 15	13, 14
	19	15.6	0.84 d (7.2)	12	11, 12, 13	12, 13, 16
MoCys1	20	173.3				
	21	84.7				
	22a	41.1	3.82 m	22b	20, 21, 24	
	22b		3.15 d (11.3)	22a	20, 21, 24	23
	23	25.6	1.55 s		20, 21, 22	13, 14, 13-OH, 14-NH, 22a, 22b
MoCys2	24	176.2				
	25	83.4				
	26a	42.8	3.52 d (11.2)	26b	24, 25, 28	27
	26b		3.43 d (11.2)	26a	24, 25, 28	27
	27	24.1	1.61 s		24, 25, 26	26a, 26b
MoCys3	28	161.7				
	29	147.7				
	30	122.8	7.94 s		28, 29, 31	
Dmetua	31	165.8				
	32	33.2	2.98 d (7.8)	33	31, 33	35, 44
	33	79.3	3.79 m	32, 34	31, 35, 45	35, 44, 45
	34	35.8	2.35 m	33, 35, 44	33, 35	36, 43, 45
	35	75.2	5.18 d (9.7)	34	1, 33, 34, 36, 37, 43	32, 33, 37, 38, 44, 37-OH
	36	38.2	1.72 m	37, 43	37	34, 38, 42, 37-OH
	37	72.2	3.18 d (8.4)	36, 38	35	3, 35, 39a, 39b, 43
			OH, 3.97 d (6.0)		37	35, 36, 39a, 39b, 42
	38	33.7	1.49 m	37, 39a, 42	40	36, 43
	39a	36.6	1.25 m	38, 39b	37	37, 37-OH
	39b		1.15 d (6.3)	38	37	37
	40	20.0	1.24 m			
	41	14.4	0.831 t (6.9)		39, 40	
	42	12.0	0.73 d (6.7)	38	37, 39	36, 39a, 37-OH
	43	9.9	0.82 d (6.8)	36	35, 36, 37	3, 34, 37. 38
	44	10.5	0.86 d (7.2)	34	33, 35	33, 35
	45	56.8	3.24 s		33	33, 34

[a] From ^{1}H to the indicated ^{13}C.

between H-19 and H-13/H-14 led to the assignment of the relative configuration of C-12−C-13 as an *erythro* rotamer B-3. The small homonuclear and heteronuclear coupling constants between H-13/H-14, H-13/C-15, and H-12/C-14 were indicative of the relative configuration between C-13−C-14 being the threo rotamer A-1, and this was consistent with a series of ROESY correlations (H-12/H-14, H-14/H-13, H-13/H-15, H-15/OH-13, and OH-13/NH-14). The relative configuration of C-14/C-15 was assigned as an *erythro* rotamer B-3 by the large *J* value between H-14 and H-15 ($^3J_{\text{H-14, H-15}} = 9.7$ Hz) and another series of ROESY correlations (H-14/H-18, H-18/H-13, H-13/H-15, and H-15/14-NH).

On the basis of the large coupling constants between H-33/H-34, H-34/H-35, and H-36/H-37, in combination with ROESY correlations between the protons associated with these adjacent chiral centers, C-33/C-34, C-34/C-35, and C-36/C-37 were assigned as *erythro* rotamers B-3. The remaining two pairs of methine centers, namely, C-35/C-36 and C-37/C-38, possessed small $^3J_{HH}$ and large $^3J_{HC}$ couplings ($^3J_{\text{H-35C-43}} = 8.7$ Hz; $^3J_{\text{H-37C-42}} = 8.8$ Hz), and thus their configurations were both assigned as *threo* rotamers A-1.

Observation of ROESY correlations between protons of the Ahdhe unit and MoCys1, the latter of which was now of assigned absolute configuration, allowed identification of the four stereocenters present in the Ahdhe unit. Specifically, the exchangeable proton NH-14 correlated with two methine protons of the Ahdhe unit (H-12 and H-14) as well as the methyl singlet (H-23) of MoCys1. Thus, the absolute configuration of the Ahdhe unit was deduced as 12*R*, 13*S*, 14*S*, and 15*S*.[8]

The absolute configuration of the Dmetua portion was revealed by analysis of the Mosher esters produced by esterification of the C-37 hydroxy group of hoiamide B (**2**). However, the Mosher esterification reactions that yielded the 37-(*S*/*R*)-MTPA esters were

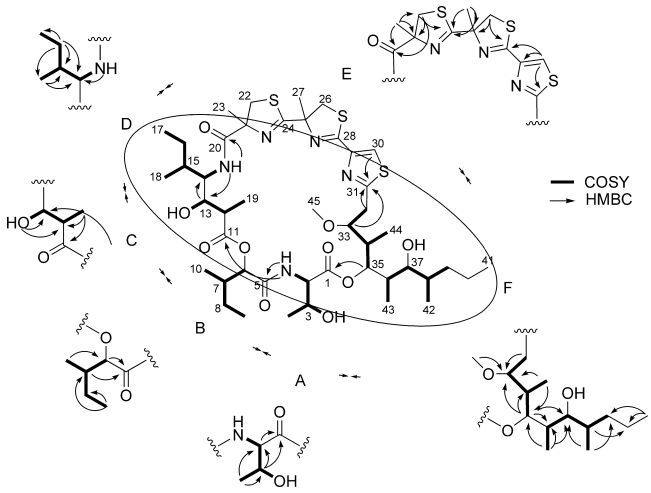

Figure 2. Partial structures of hoiamide B (**2**) derived from 2D NMR data and their assembly by key HMBC correlations.

accompanied by dehydration of the threonine residue, producing the 2,3-dehydrohoiamide B derivatives **6** and **7**. Calculation of Δ_{S-R} values around C-37 allowed assignment of its absolute configuration as *S*, and thus, the absolute configuration of the Dmetua residue was determined as 33*S*, 34*S*, 35*R*, 36*S*, 37*S*, and 38*R* (Figure 4).

Isolation, Structure Elucidation, and Semisynthesis of Hoiamide C (3). A second mixed collection of marine cyanobacteria, obtained by scuba on a reef wall near Pigeon Island, Papua New Guinea, was extracted repeatedly with CH_2Cl_2−MeOH (2:1) and then fractionated by silica gel vacuum-column chromatography (VLC) to produce nine fractions (A−I). The F fraction, eluting with 80% EtOAc−hexanes, was found to possess potent brine shrimp toxicity (LC_{50}, ca. 5 μg/mL). This material was thus subjected to RP HPLC and yielded a small quantity of hoiamide C (**3**, 2.9 mg, 0.02%). Pure hoiamide C (**3**) exhibited an LC_{50} of 1.3 μM in the brine shrimp toxicity assay.

LRESIMS of hoiamide C (**3**) yielded an $[M + H]^+$ peak at *m/z* 771.22 as part of a complex isotopic pattern [*m/z* 771/772/773/774/775 (100:52:26:11:5)] and thus suggested once again the presence of three sulfur atoms as in hoiamide A (**1**). This interpretation was confirmed by HREIMS of **3**, which gave a molecular ion peak at *m/z* 770.3743 for a molecular formula of $C_{37}H_{62}N_4O_7S_3$ (calcd 770.3775) with nine degrees of unsaturation. IR absorptions at 3389 (broad), 1731, and 1656 (broad) cm^{-1} were consistent with the presence of hydroxy, ester, and amide functionalities, respectively. Furthermore, a UV absorption maximum at 250 nm was essentially identical to that measured for hoiamides A (**1**) and B (**2**). On combining this information with a complete NMR data set for **2** (Table 2), it was clear that compound **3** was related to hoiamides A (**1**) and B (**2**), but of an overall truncated size.

The ^{1}H NMR spectrum of **3** (pyridine-d_5) possessed resonances for a methoxy singlet at δ_H 3.32, three methyl triplets at δ_H 1.11, 0.91, and 0.87, five methyl doublets between δ_H 1.32 and 0.93, and multiple oxymethine resonances between δ_H 4.50 and 2.50, suggesting polyketide-derived substructures closely related to Ahdhe and Dmetua. Additionally, two methyl singlets at δ_H 2.03 and 1.75, as well as an aromatic proton singlet at δ_H 8.27, confirmed the presence of a cysteine-based triheterocyclic ring system as found in hoiamides A (**1**) and B (**2**). Extensive analysis by HSQC, HMBC, COSY, and z-TOCSY experiments revealed the planar structure of a new linear hoiamide analogue, named hoiamide C (**3**).

A first inspection of the HMBC data involved analysis of long-range correlations to the various methyl group protons, each of which showed a full complement of two- and three-bond correlations with their neighboring carbon atoms, and led to the identification of partial structures A−E (Figure 5). Additional connections were made by COSY, such as between C-3 and C-4, as revealed by correlations between H-3 (δ_H 4.43) and H-4 (δ_H 4.13). An HMBC correlation between H-36 (δ_H 4.17/4.11) and C-1 (δ_C 176.3), along with the chemical shift of C-36 (δ_C 60.5), indicated the presence of an ester linkage between C-1 and C-36. The chemical shifts of C-3 (δ_C 71.7), C-23 (δ_C 81.8), C-25 (δ_C 71.6), and C-27 (δ_C 76.4) suggested directly linked oxygen atoms to each of these methines. In contrast, the chemical shift of C-4 (δ_C 54.1) was more appropriate for a nitrogen-linked carbon, and this was confirmed by observation of vicinal coupling between the NH doublet at δ_H 7.57 (NH at C-4) and the methine proton at δ_H 4.13 (H-4) by COSY. In addition, HMBC correlations involving both the NH proton (δ_H 7.57) and H-4 (δ_H 4.13) with the carbonyl carbon atom C-10 (δ_C 174.7) suggested an adjacent amide functional group.

Structure elucidation of the central triheterocyclic partial structure of compound **3** was greatly facilitated by a combination of HMBC and ^{15}N HMBC experiments. The H-13 methyl protons, resonating as a singlet at δ_H 1.75, exhibited HMBC correlations with the amide carbon atom C-10 (δ_C 174.7), a quaternary carbon atom at δ_C 85.7 (C-11), and a methylene carbon atom at δ_C 41.9 (C-12). In addition, an ^{15}N HMBC experiment displayed a correlation between H_3-13 and a nitrogen atom resonating at δ_N −76.1 (see Supporting Information). The chemical shift of protons at C-12 (δ_H 4.18/3.31) suggested an adjacent heteroatom, which, on the basis of the chemical shift of C-12 (δ_C 41.9), was deduced to be a sulfur atom. Both protons at C-12 showed reciprocal HMBC correlations with C-13 and C-11 and also with a quaternary sp^2 carbon atom at δ_C 178.9 (C-14). The deshielded chemical shift of the latter carbon atom suggested a link with the δ_N −76.1 nitrogen atom and thus described a methylthiazolene ring. Likewise, HMBC correlations of H_3-17 (δ_H 2.03) with C-14 (δ_C 178.9), C-15 (δ_C 85.0), C-16 (δ_C 43.0), and a second nitrogen at δ_N −70.7, as well as those of H_2-16 (δ_H 4.13/3.52) with C-17 (δ_C 27.0), C-14 (δ_C 178.9), C-15 (δ_C 85.0), and C-18 (δ_C 163.5), were indicative of a second methylthiazolene ring. The last heterocycle in the system, a thiazole ring, was indicated by HMBC correlations of the aromatic proton H-20 (δ_H 8.27) with C-18 (δ_C 163.5), C19 (δ_C 148.3), and C-21 (δ_C 170.4). With this latter thiazole ring described, all of the required degrees of unsaturation were satisfied. COSY provided evidence of vicinal coupling between H-23 (δ_H 4.41) and both diastereotopic protons at H_2-22 (δ_H 3.49/3.13); in turn, these methylene protons also displayed HMBC correlations with the sp^2 carbon atom at δ_C 170.4 (C-21) of the adjacent thiazole ring. These latter connections linked the triheterocyclic ring portion with the polyketide section and thus completed the planar structure of hoiamide C (**3**) (Figure 5).

Owing to the limited quantity of hoiamide C (**3**) at this point in the structure elucidation, we prioritized evaluation of its biological properties over chemical degradation studies. However, we envisioned a possible semisynthetic strategy to produce **3** from hoiamide A (**1**) via regioselective hydrolysis of both ester bonds using LiOH, followed by esterification of the resulting free carboxylic acid with ethanol in the presence of catalytic HCl (Figure 6a). This sequence of reactions was performed with hoiamide A (**1**), and the resulting semisynthetic compound proved to be identical by ^{1}H and ^{13}C NMR (Figure 6b), IR, UV, MS, and HPLC comparison with the material extracted from *Symploca* sp., confirming the structure proposed for the natural product **3**. Furthermore, positive specific rotation values and comparable circular dichroism curves (Supporting Information) for both semisynthetic and natural hoiamide C (**3**) confirmed that both hoiamides A and C possess the same configuration at their comparable stereocenters. Thus, hoiamide C (**3**) was shown to possess 2*R*, 3*S*, 4*S*, 5*S*, 11*S*, 15*R*, 23*S*, 24*R*, 25*R*, 26*S*, 27*S*, and 28*R* absolute configuration.

Biosynthetic Prediction of Hoiamides B (2) and C (3). Hoiamides A−C (**1**−**3**) are interesting representatives of a new natural product class deriving from integration of PKS and NRPS

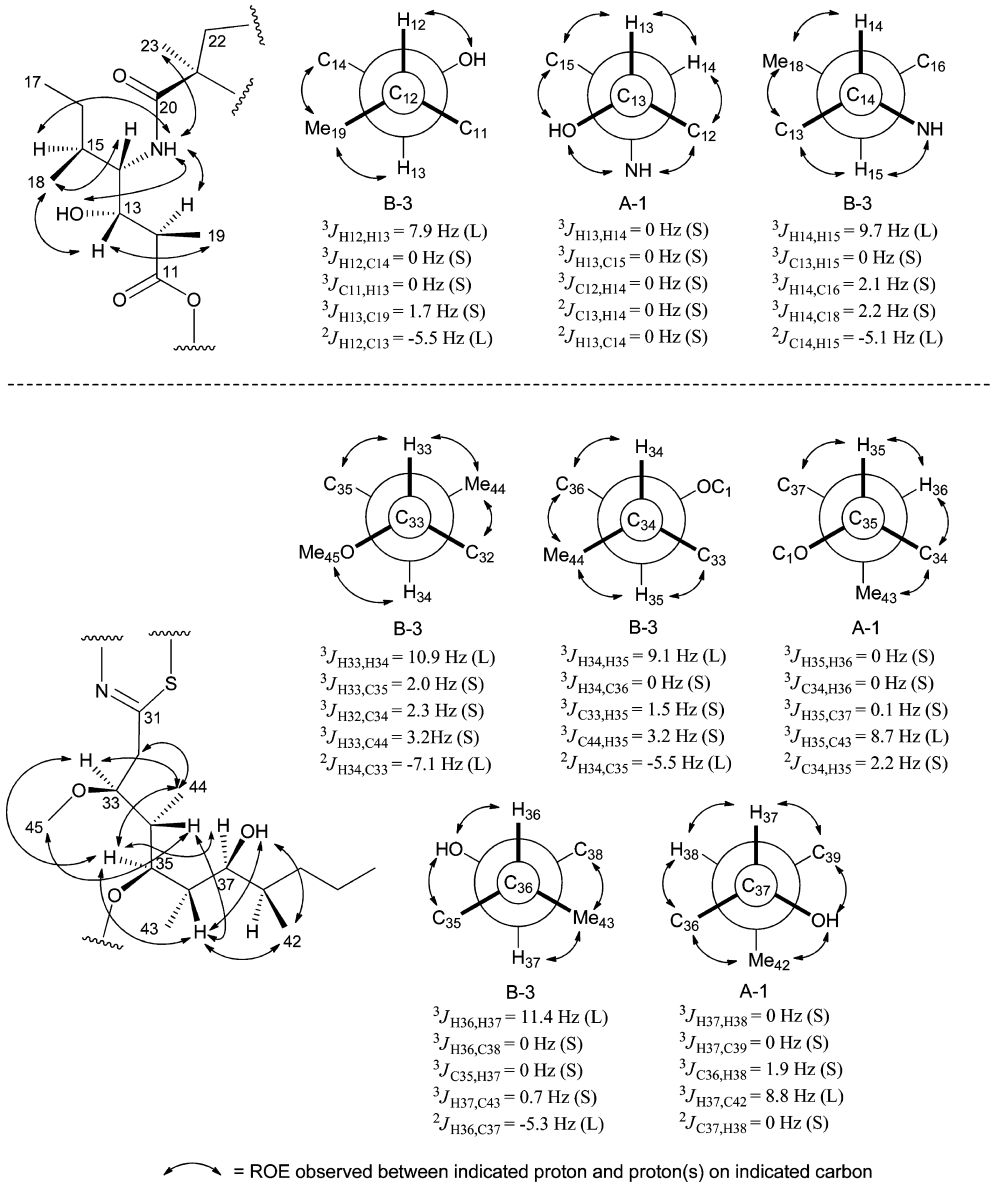

Figure 3. Depiction of homonuclear and heteronuclear coupling constants and ROE correlations used to assign the relative stereochemistry of the Ahdhe (C-11−C-19) and Dmetua (C-31−C-45) residues in hoiamide B (**2**).

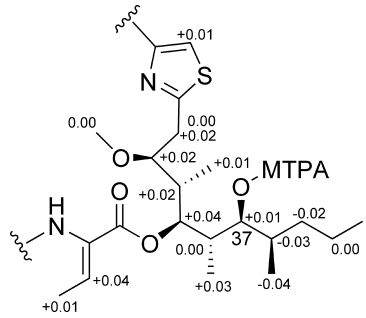

Figure 4. $\Delta\delta_{S-R}$ values around C-37 of the Mosher esters of hoiamide B (**6** and **7**).

biosynthetic pathways. The Dmetua residue is a highly oxidized and branched polyketide chain and is predicted to be the initial biosynthetic unit formed in the hoiamides. The remnant oxidations on the chain are likely reflections of C-1 positions in the acetate subunits. Conversely, the methyl groups all occur at predicted C-2 positions of the acetate subunits and thus are likely incorporated from the methyl group of *S*-adenosyl methionine (SAM). Perhaps most interesting in this section of the molecule is the observation that the Dmetua fragment consists of an 11-carbon unbranched chain. While conceivably deriving from a propionate starter unit followed by four acetate extensions (from malonyl CoA), its origination from SAM methylation of a acetate starter unit is favored because (a) utilization of propionate is essentially unknown in cyanobacterial polyketides[10] and (b) there is precedence for this type of transformation from biosynthetic labeling experiments with homoanatoxin A[11] as well as unpublished work on apratoxin A biosynthesis in our laboratory. The three consecutive heterocyclic rings are likely created from three cysteine residues by heterocyclization followed by either dehydration to form the thiazole or stereoselective methylation of the α-carbon to produce the two α-methyl thiazolines. Following this section is the Ahdhe fragment, which is likely created from an isoleucine residue extended by an acetate unit. In this case, it is predicted that the C-2 position of the acetate unit is methylated by SAM followed by reduction of the carbonyl group to a secondary alcohol.[5] While the Ahdhe residue of hoiamide C (**3**) is capped as the ethyl ester (possibly an artifact from EtOH extraction), in hoiamides A (**1**) and B (**2**) this group is extended by connection to the hydroxy acid hydroxyisovaleric acid (Hiva) or hydroxymethylpentanoic acid (Hmpa), respectively. From

Table 2. NMR Spectroscopic Data for Hoiamide C (**3**) in Pyridine-d_5 at 700 MHz (^{1}H) and 175 MHz (^{13}C)

residue	position	δ_C[a]	δ_H mult (*J* in Hz)	COSY	HMBC[b]	ROESY
Ahdhe	1	176.3				
	2	45.3	2.90, m	3, 9	1, 3	3
	3	71.7	4.43, br d (9.7)[c]	2, 4		2, 4, 8, 9
	4	54.1	4.13, br t (9.7)[c]	3, 5, NH	5, 8, 10	3, 8, 9, NH
			NH 7.57, d (9.7)	4	10	4
	5	36.7	2.00, m	4, 8		
	6a	26.4	1.76, m	6b, 7		6b
	6b		1.37, m	6a, 7	7, 8	6a, 8
	7	11.5	0.91, t (7.5)	6a, 6b	5, 6	
	8	16.0	0.95, d (6.7)	5	4, 5, 6	3, 4, 6b
	9	14.7	1.32, d (7.0)	2	1, 2, 3	3, 4
MoCys1	10	174.7				
	11	85.7				
	12a	41.9	4.18, d (11.5)	12b	10, 11, 13, 14	12b
	12b		3.31, d (11.5)	12a	10, 11, 13, 14	12a, 13
	13	26.5	1.75, s		10, 11, 12	12b
MoCys2	14	178.9				
	15	85.0				
	16a	43.0	4.13, d (11.3)	16b	14, 15, 17, 18	16b
	16b		3.52, d (11.3)	16a	14, 15, 17, 18	16a, 17
	17	27.0	2.03, s		14, 15, 16	16b
MoCys3	18	163.5				
	19	148.3				
	20	122.1	8.27, s		18, 19, 21	
Dmetua	21	170.4				
	22a	34.2	3.49, dd (15.4, 2.2)	22b, 23	21	22b, 23, 25
	22b		3.13, dd (15.4, 10.6)	22a, 23	21, 23	22a, 34
	23	81.8	4.41, ddd (10.6, 3.5, 2.2)	22a, 22b, 24		24, 35
	24	37.4	2.50, m	23, 25, 34		23, 33, 34, 35
	25	71.6	4.39, dd (10.3, 1.3)	24, 26	26, 33, 34	22a, 26, 27, 28
	26	37.9	2.03, m	25, 27, 33	27, 33	25, 27, 32, 34
	27	76.4	3.90, dd (7.1, 4.5)	26, 28	25, 26, 29, 32	25, 26, 28, 29a, 29b, 33
	28	35.5	1.86, m	24, 29a, 29b, 32	29	25, 27, 33
	29a	37.3	1.57, m	28, 29b, 30	30	27, 29b
	29b		1.36, m	28, 29a	30	27, 29a
	30	20.8	1.37, m	29a, 31	29	
	31	14.9	0.87, t (7.0)	30	29, 30	
	32	14.2	1.14, d (6.7)	28	27, 28, 29	26
	33	10.5	1.19, d (6.9)	26	25, 26, 27	24, 27, 28
	34	10.4	0.93, d (7.0)	24	22, 24, 25	22b, 24, 26
	35	56.8	3.32, s		23	23, 24
	36a	60.5	4.17, m	36b, 37	1	
	36b		4.11, m	36a, 37		
	37	14.6	1.11, t (7.1)	36a, 36b	36	

[a] Derived from HSQC and HMBC data. [b] From ^{1}H to the indicated ^{13}C. [c] Multiplicity from the z-TOCSY spectrum.

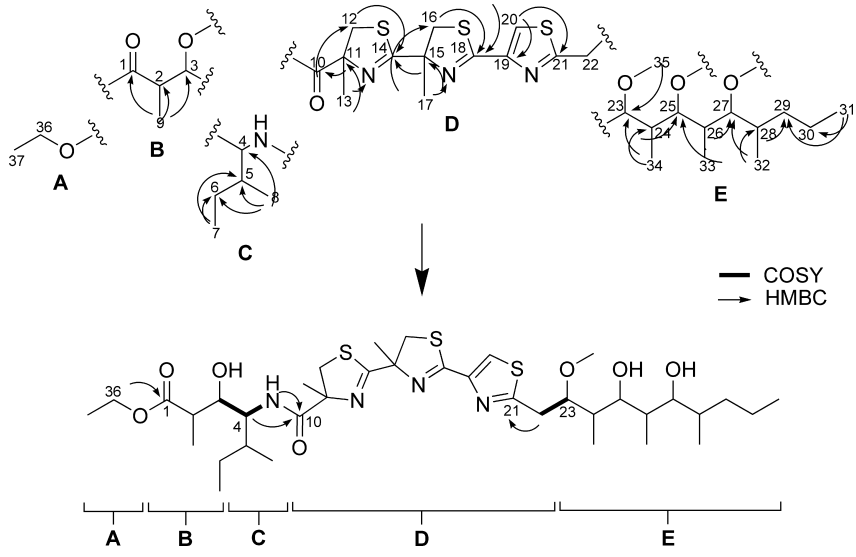

Figure 5. Selected HMBC, ^{15}N HMBC, and COSY correlations involved in building and interconnecting partial structures A−E of hoiamide C (**3**).

our genetic work with the hectochlorin biosynthetic pathway, it is predicted that these two residues are selected initially for incorporation as the corresponding α-keto acids and then reduced while tethered to the corresponding peptidyl carrier protein (PCP).[12] The

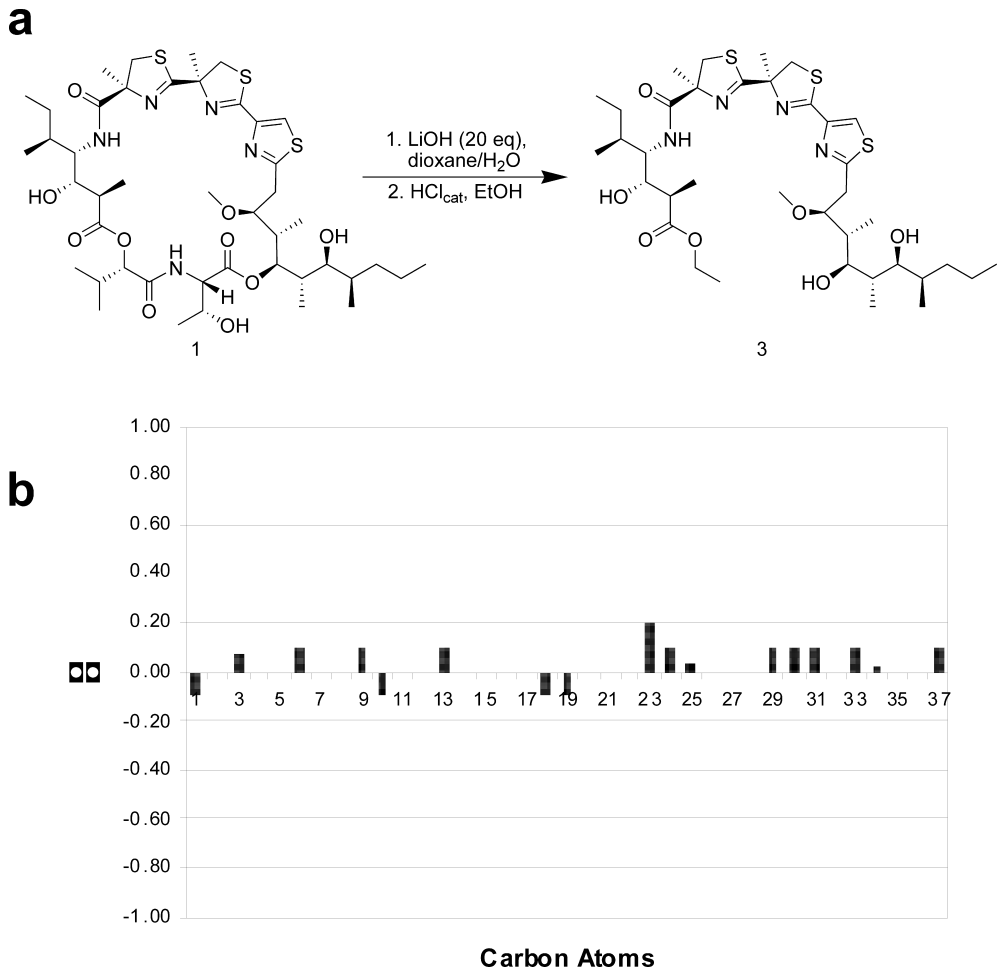

Figure 6. (a) Route for the semisynthesis of hoiamide C (**3**) from hoiamide A (**1**); (b) $\Delta\delta_C$ of natural and semisynthetic hoiamide C (**3**).

predicted pathways to both hoiamides A (**1**) and B (**2**) conclude with incorporation of the standard amino acid, L-threonine. Finally, the hydroxy group at C-35 in the Dmetua portion of hoiamide B (C-34 in hoiamide A) likely participates in a thioesterase-mediated hydrolysis of the chain from the final PCP with coincident lactonization, thereby forming the 26-membered macrocyclic ring.

Taxonomy of the Hoiamide-Producing Cyanobacterial Strains. The two cyanobacteria that produced hoiamides B (**2**) and C (**3**) were taxonomically compared with the hoiamide A (**1**)-producing strain. Hoiamide A (**1**) was originally isolated from a consortium of two different filamentous cyanobacteria identified as *Lyngbya majuscula* (Harvey *ex* Gomont) and *Phormidium gracile* (Meneghini *ex* Gomont) on the basis of morphology.[8] This cyanobacterial assemblage was predominantly composed of fine *Phormidium* filaments entangled into thick pads that contained embedded thicker, reddish *Lyngbya* filaments. As a result of these entangled filaments, this *Phormidium/Lyngbya* consortium formed extensive mats with cespitose short purple tufts. The hoiamide B (**2**)-producing cyanobacterium, PNG06-64, was collected as dark brownish-red mats covering the coral reefs, and its overall growth morphology resembled that of the hoiamide A producer (Figure 7a). Interestingly, the hoiamide C producer possessed a distinctly different thallus morphology compared with the hoiamide A and B producers. The hoiamide C producer formed erect bundles of a brownish-red purple color (Figure 7b).

Microscopically, the three different hoiamide producers appeared similar, with the vast majority of the biomass composed of fine entangled filaments (7−10 μm) with isodiametric or slightly longer cells. This description corresponds with the *Phormidium* morpho-type previously described from the hoiamide A producer (Figure 7c,d). Embedded in the *Phormidium* of the hoiamide A and B producers were also wider reddish filaments with disk-shaped cells surrounded by distinct sheaths, which corresponded with the *Lyngbya* morpho-type (Figure 7c inset).

The hoiamide B and C producers were phylogenetically analyzed on the basis of their SSU (16S) rRNA genes to obtain a better understanding of their evolutionary relationships and taxonomic positions. The resulting phylogenies revealed that the *Phormidium* morpho-types are related evolutionarily to various specimens of *Symploca*, including the type-strain PCC 8002 and, thus, should be reclassified as *Symploca.* The morphologically similar genera *Phormidium* and *Symploca* both belong to the family Phormidiaceae (Anagnostidis *et* Komárek, 1998) and are distinguished traditionally by their thallus morphology. According to these systems, the hoiamide A and B producers formed mats corresponding with the definition of *Phormidium*, while the hoiamide C producer formed erect bundles corresponding to the genus *Symploca.* However, our phylogenetic analysis revealed that both the hoiamide B and C producers belong to the genus *Symploca*, and it is suggested that this traditional diacritical feature is taxonomically uninformative and needs to be reconsidered. Along the same lines, the *Lyngbya* morpho-type present in the mat producing hoiamide B was found by 16S rRNA analysis to be closely related to the *Oscillatoria* type-strain PCC 7515. Thus, while these two latter genera can have very similar overall morphologies, our genetic analysis reveals the thicker filaments in the mat to be *Oscillatoria*.

Whether the biosynthesis of the hoiamides occurs in *Oscillatoria* or *Symploca* can only be speculated upon at this point. The fact that *Symploca* was the major component of all three samples and that *Oscillatoria* was present only in the hoiamide A (**1**) and B (**2**)

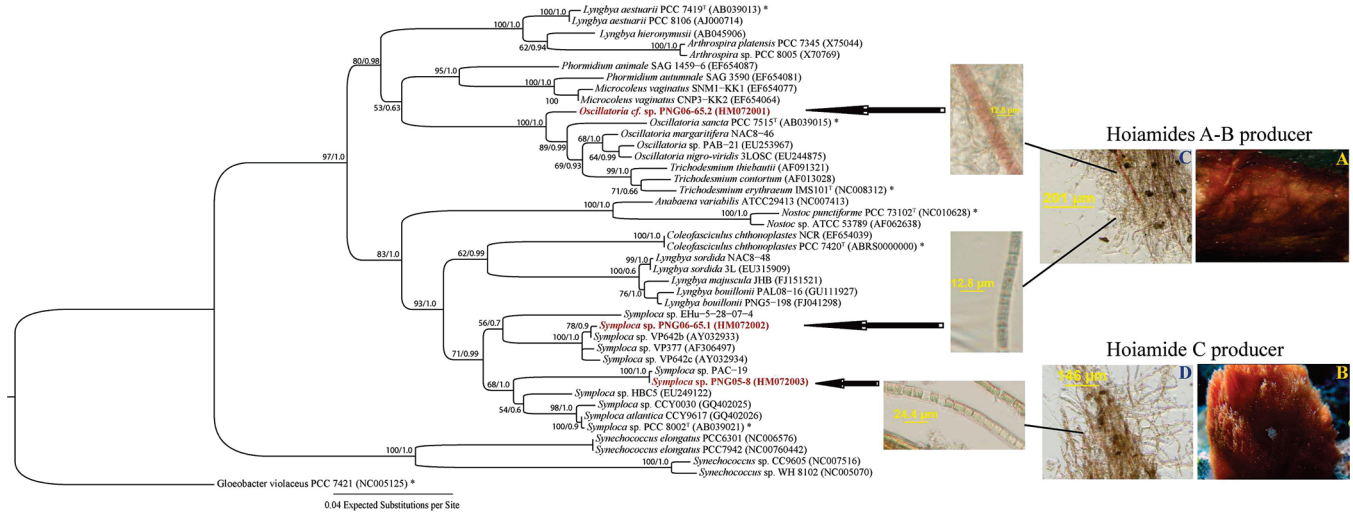

Figure 7. Maximum-likelihood (PhyML) phylogenetic analysis of the hoiamide-producing cyanobacteria based on SSU (16S) rRNA nucleotide sequences. The specimens are indicated as species, strain, and acc. nr in brackets. Specimens designated with an asterisk represent type-strains obtained from *Bergey's Manual.* The support values are indicated as boot-strap (PhyML) and posterior probability (MrBayes). The scale bar is indicated at 0.04 expected nucleotide substitutions per site. Underwater field images of (A) the hoiamides A and B producer and (B) the hoiamide C producer. Microscopic images of (C) hoiamides A and B and (D) hoiamide C producer.

Table 3. Biological Activities of Naturally Occurring Hoiamides A−C (**1**−**3**) and Derivatives **4** and **5**

	inhibition of Ca^{2+} oscillations[a]	activation of VGSC[a]	H-460[b]	Neuro-2a[c]
compound	(IC_{50} nM, 95% CI)	(IC_{50} μM, 95% CI)	(IC_{50} μM)	(IC_{50} μM)
1	45.6 (30.3−68.6)	1.7 (0.7−4.2)	11.2	2.1[c]
2	79.8 (29.5−215.5)	3.9 (1.2−13.0)	8.3	inactive
3	inactive	inactive	inactive	inactive
4	87.3 (19.8−385.0)	9.3 (1.0−90.0)	Inactive	3.4[d]
5	inactive	inactive	inactive	inactive

[a] Mouse neocortical neurons. [b] Cytotoxicity to human lung adenocarcinoma cells. [c] Cytotoxicity to mouse neuroblastoma cells. [d] VGSC activation in mouse neuroblastoma cells.

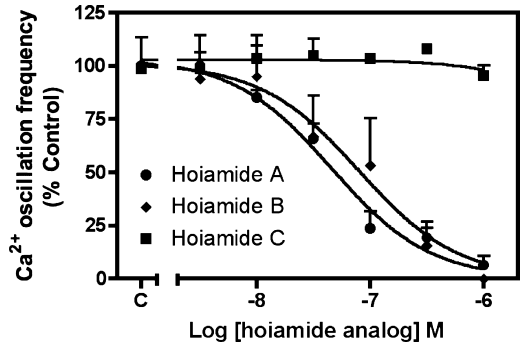

Figure 8. Concentration−response relationships for suppression of spontaneous Ca^{2+} oscillations in neocortical neurons by various hoiamide analogues.

producers suggest that *Symploca* is likely the origin of these unusual metabolites. However, conflicting with this hypothesis is the considerable evolutionary distance between the *Symploca* specimens present in these three samples. In this regard, it is conceivable that an *Oscillatoria* spp. was originally present in the hoiamide C-producing collection, but that it was not observed due to the small size of the retained voucher sample.

Bioactivity of the Hoiamides. The biological properties of hoiamides A−C (**1**−**3**) as well as two semisynthetic derivatives (compounds **4** and **5**) are summarized in Table 3. Both hoiamides A (**1**) and B (**2**) stimulated sodium influx with EC_{50} values of 1.7 and 3.9 μM, respectively, in mouse neocortical neurons. Previously, we have demonstrated that hoiamide A is a sodium channel neurotoxin site 2 partial agonist.[8] Given the structural similarity between hoiamides A and B and comparable ability to stimulate sodium influx, it is reasonable to conclude that hoiamide B is also a site 2 sodium channel activator. Additionally, hoiamides A (**1**) and B (**2**) were both found to potently suppress spontaneous calcium oscillations in neocortical neurons with EC_{50} values of 45.6 and 79.8 nM, respectively (Figure 8). The effects of hoiamides A and B on spontaneous calcium oscillations are therefore of greater potency than their respective effects on sodium influx. This inhibitory effect on spontaneous calcium oscillations is not related to their ability to activate voltage-gated sodium channels, inasmuch as sodium channel activators actually enhance calcium oscillation amplitude and frequency in low concentrations and produce a sustained elevation of cytoplasmic calcium concentration at higher concentrations.[13] Synchronized Ca^{2+} oscillations in neurons in culture is considered to be a neuronal network phenomenon that is dependent on voltage-gated sodium channel mediated action potentials.[14] Although the mechanism(s) underlying hoiamide A (**1**) and B (**2**) induced inhibition of calcium oscillations is presently unknown, these natural products may disrupt the neurotransmission that drives a neuronal network function. Interestingly, switching from a Hiva residue in **1** to a Hmpa residue in **2** significantly decreased cytotoxicity levels in the Neuro-2a neuroblastoma cell line. The linear analogue hoiamide C (**3**) and the cyclic triacetylated derivative (**5**), however, showed no significant pharmacological activity in these assays, clearly suggesting that the macrocycle and its hydrogen bond donors at C-3, C-13, and C-37 in **1** and **2** play a key role in their interactions with molecular targets. This is also true for analogue **4**, which additionally shows that modifying the alkyl side chain by esterification of the C-37 hydroxy group of hoiamide A (**1**) decreases cytotoxicity significantly (no cytotoxicity observed up to 27.0 μM) and thus allowed a low micromolar VGSC activation to be measured for this derivative in mouse neuroblastoma cells (IC_{50} 3.3 μM). This result correlates with the VGSC activation measured in mouse neocortical neurons (IC_{50} 9.3 μM) and suggests that the hoiamides may have more than one molecular target in cells that separately involve suppression of Ca^{2+} oscillations and VGSC activation.

Experimental Section

General Experimental Procedures. Optical rotations were measured on a JASCO P-2000 polarimeter, UV spectra on a Beckman Coulter DU800 spectrophotometer, and IR spectra on a Nicolet ThermoElectron

Nicolet IR100 FT-IR spectrometer using KBr plates. NMR spectra were recorded with DMSO (δ_C 39.5, δ_H 2.50), pyridine (δ_C 150.3, δ_C 135.9, δ_C 123.9, δ_H 8.73, δ_H 7.56, δ_H 7.21), or chloroform as internal standards (δ_C 77.2, δ_H 7.26), on a Bruker 600 MHz spectrometer (600 and 150 MHz for ^{1}H and ^{13}C NMR, respectively), equipped with a 1.7 mm MicroCryoProbe or a Varian 700 MHz spectrometer (700 and 175 MHz for ^{1}H and ^{13}C NMR, respectively) with a 5 mm HCN cold probe. ^{15}N NMR spectra were referenced to CH_3NO_2 from the observed dimension. LR- and HRESIMS were obtained on a ThermoFinnigan LCQ Advantage Max mass detector and Agilent 6200 ESI-TOF mass spectrometer, respectively. HREIMS spectra were obtained also on a ThermoFinnigan MAT900XL mass spectrometer. HPLC was carried out using a Waters 515 pump system with a Waters 996 PDA detector.

Cyanobacterial Collections and Taxonomic Identification. The hoiamide B (**2**)-producing cyanobacterium (collection code: PNG-4-28-06-1) was collected by scuba at a depth of 15−18 m at the Gallows Reef of Papua New Guinea, in April 2006 (150°44.878′ E, 10°15.612′ S). The hoiamide C (**3**)-producing cyanobacterium (collection code: PNG-5-19-05-7) was collected by scuba on a 10 m deep reef wall near Pigeon Island, Papua New Guinea, in May 2005 (152°20.266′ E, 4°16.0.63′ S). Morphological characterization was performed using an Olympus IX51 epifluorescent microscope (100×) equipped with an Olympus U-CMAD3 camera. Taxonomic identification of cyanobacterial specimens was performed in accordance with current phycological systems.[15]

Polymerase Chain Reaction (PCR) and Cloning. Approximately 50 mg of algal biomass was cleaned and pretreated using TE (10 mM Tris; 0.1 M EDTA; 0.5% SDS; 20 μg/mL RNase)/lysozyme (1 mg/mL) at 37 °C for 30 min followed by incubation with proteinase K (0.5 mg/mL) at 50 °C for 1 h. Genomic DNA was extracted using the Wizard Genomic DNA purification kit (Promega Inc., Madison, WI) following the manufacturer's specifications. DNA concentration and purity were measured on a DU 800 spectrophotometer (Beckman Coulter). The 16S rRNA genes were PCR-amplified from isolated DNA using the modified lineage-specific primers, 106F 5′-CGGACGGGTGAGTAACGCGTGA-3′ and 1509R 5′-GGCTACCTTGTTACGACTT-3′/1445R 5′-GGTAACGACTTCGGGCGTG-3′. The PCR reaction volumes were 25 μL containing 0.5 μL (∼50 ng) of DNA, 2.5 μL of 10 × PfuUltra IV reaction buffer, 0.5 μL (25 mM) of dNTP mix, 0.5 μL of each primer (10 μM), 0.5 μL of PfuUltra IV fusion HS DNA polymerase, and 20.5 μL of H_2O. The PCR reactions were performed in an Eppendorf Mastercycler gradient as follows: initial denaturation for 2 min at 95 °C, 25 cycles of amplification, followed by 20 s at 95 °C, 20 s at 50 °C, and 1.5 min at 72 °C, and final elongation for 3 min at 72 °C. PCR products were purified using a MinElute PCR purification kit (Qiagen) before subcloning using the Zero Blunt TOPO PCR cloning kit (Invitrogen) following the manufacturer's specifications. Plasmid DNA was isolated using the QIAprep spin miniprep kit (Qiagen) and sequenced with M13 primers. The 16S rRNA gene sequences are available in the DDBJ/EMBL/GenBank databases under acc. nos. HM072001−HM072003.

Phylogenetic Inferences. All gene sequences were aligned using MUSCLE v4.0[16] and refined using the SSU secondary structures model for *Escherichia coli* J01695.[17] Best-fitting nucleotide substitution models optimized by maximum likelihood were selected using corrected Akaike/Bayesian Information Criterion (AIC/BIC) in ModelTest 3.7.[18] The evolutionary histories of the cyanobacterial genes were inferred using maximum likelihood (ML) and Bayesian inference algorithms. The maximum likelihood inference was performed using PhyML v2.4.4.[19] The analysis was run using the GTR+I+G model (selected by AIC and BIC) assuming a heterogeneous substitution rate and gamma substitution of variable sites (proportion of invariable sites (pINV) = 0.529, shape parameter (α) = 0.453, number of rate categories = 4). Bootstrap resampling was performed on 500 replicates. Bayesian analysis was conducted using MrBayes 3.1.[20] The Bayesian inference was performed using the GTR+I+G substitution model (pINV = 0.450, α = 0.449, number of rate categories = 4) with Markov chains (one cold and three heated) ran for 3 000 000 generations. The first 25% were discarded as burn-in and the following data set were being sampled with a frequency of every 100 generations. The MCMC convergence was detected by AWTY.[21]

Isolation of Hoiamide B (2). The cyanobacterial tissue (141 g, dry wt) was extracted repetitively with 2:1 CH_2Cl_2−MeOH to afford 900 mg of crude extract. A portion of the extract (761 mg) was fractionated by silica gel VLC with a stepwise gradient solvent system of increasing polarity starting from 10% EtOAc in hexanes to 100% MeOH, to produce nine fractions (A−I). The fraction eluting with 80% EtOAc in hexanes (fraction F) was separated subsequently using RP HPLC (Phenomenex Jupiter 10 μm C_{18}, 250 × 10 mm, 85% MeOH−H_2O at 3 mL/min, detection at 228, 254, and 280 nm) to give pure hoiamide A (**1**, 21 mg, 2.8%) and hoiamide B (**2**, 8.9 mg, 1.2%).

Hoiamide B (2): pale yellow oil; $[\alpha]^{25}_D$ +5.0 (*c* 0.3, $CHCl_3$); UV (MeCN) λ_{max} 250 nm (log ε 3.86); IR (KBr) ν_{max} 3386, 2966, 2933, 1742, 1672 cm^{-1}; ^{1}H, ^{13}C, and 2D NMR data, see Table 1; HRESIMS *m/z* $[M + H]^+$ 940.4584 (calcd for $C_{45}H_{73}N_5O_{10}S_3$ 940.4598).

Acid Hydrolysis and Marfey's Analysis.[22] Hoiamide B (**2**, 150 μg) was treated with 150 μL of 6 N HCl at 110 °C for 30 min. The reaction product was obtained by lyophilization, and the residue was dissolved in 150 μL of water. An aliquot (100 μL) of the resuspended residue was transferred into a 1.5 mL glass vial and dried. The dried hydrolysate was dissolved in 100 μL of 1 M sodium bicarbonate, and then 25 μL of 1% L-FDLA (1-fluoro-2,4-dinitrophenyl-5-L-leucine amide) was added in acetone. The solution was vortexed and incubated at 40 °C for 60 min. The reaction was quenched by the addition of 50 μL of 2 N HCl, and then the reaction mixture was diluted with 100 μL of MeOH and 10 μL of the solution was analyzed by LC-ESIMS.

The reaction products from advanced Marfey's method were separated on a RP HPLC column (Phenomenex Jupiter 5 μm C_{18} column, 4.6 × 250 mm, 5.0 μm) with a stepped gradient elution of 0.1% TFA in water (eluent A) and 100% MeCN (eluent B). Gradient program: 0−5 min, B, 30%; 5−25 min, B, 30−70%; 25−30 min, B, 70%; 30−35 min, B, 100%; flow rate, 500 μL/min. The column temperature was kept at 30 °C. The amino acids, derivatized with advanced Marfey's reagents, were detected using ESIMS. The retention times of authentic amino acid L-FDLA derivatives were L-Thr (19.63 min), L-*allo*-Thr (20.45 min), D-*allo*-Thr (21.45 min), and D-Thr (23.05 min).

Preparation and Chiral Analysis of 2-Hydroxy-3-methylpentanoic Acid (Hmpa).[9] L-Ile (20 mg) was dissolved in 5 mL of cold (0 °C) 0.2 N $HClO_4$, and then 2 mL of $NaNO_2$(aq) was added with rapid stirring. The reaction mixture was stored at room temperature until evolution of N_2 subsided (1 h). The solution was boiled for 3 min, cooled to room temperature, and then saturated with NaCl. The mixture was extracted three times with Et_2O, and the Et_2O layer was then dried under N_2 (g) to give 17.3 mg of the oily 2*S*,3*S*-Hmpa. Correspondingly, 2*R*,3*R*-Hmpa (16.2 mg), 2*S*,3*R*-Hmpa (13.1 mg), and 2*R*,3*S*-Hmpa (15.6 mg) were synthesized with the same procedure from D-Ile, L-*allo*-Ile, and D-*allo*-Ile, repectively. Each authentic stereoisomer of Hmpa was dissolved in 2 mM $CuSO_4$(aq) with retention times measured by chiral HPLC (Phenomenex, Chirex-D-penicillamine, 4.6 × 50 mm, 0.8 mL/min, 87.5% 2 mM $CuSO_4$(aq) in MeCN). The retention time of the Hmpa residue in acid hydrolysate of **2** matched with 2*S*,3*S*-Hmpa (24.1 min; 2*S*,3*R*-Hmpa, 20.9 min; 2*R*,3*S*-Hmpa, 31.6 min; 2*R*,3*R*-Hmpa, 37.0 min).

Ozonolysis, Oxidation, Acid Hydrolysis, and Chiral HPLC. A portion (800 μg) of **2** was dissolved in 2 mL of CH_2Cl_2 at room temperature, and O_3 was bubbled through the sample for 15 min. The pale blue solution was dried under N_2(g), resuspended in 200 μL of mixed oxidation solution (H_2O_2−HCOOH, 1:2), incubated at 70 °C for 20 min, and then dried under N_2(g). The products were resuspended in 200 μL of 6 N HCl and reacted at 110 °C for 2 h. The acid hydrolysates were dried under N_2 (g), dissolved in 2 mM $CuSO_4$(aq), and injected over chiral HPLC (Phenomenex, Chirex-D-penicillamine, 4.6 × 50 mm, 0.3 mL/min, 85% 2 mM $CuSO_4$(aq) in MeCN). Synthetic standards of 2*S*-methyl cysteic acid (MeCysA) and 2*R*-MeCysA were prepared by Pattenden's method.[23] The retention time of products resulting from the acid hydrolysate of **2** matched the synthetic 2*S*-MeCysA standard (9.8 min; 2*R*-MeCysA, 11.0 min).

Preparation of MTPA Ester of Hoiamide B. Duplicate samples of compound **2** (1 mg) were dried and dissolved in 1 mL of anhydrous pyridine, and a catalytic amount of DMAP (dimethylaminopyridine) was added. Separately and into each vial, 15 μL of *R*-MTPA chloride and 15 μL of *S*-MTPA chloride were added. The reaction vials were stored at 40 °C for 72 h with stirring. The acylation products were purified using RP HPLC (Phenomenex Jupiter 5 μm C_{18}, 4.6 × 250 mm, 85% MeOH−H_2O at 1 mL/min). The *m/z* values of the two diastereomeric MTPA derivatives of compound **2** were observed by ESIMS, and the ^{1}H NMR spectrum was assigned by 2D NMR experiments including TOCSY, HSQC, and HMBC.

37-*S*-MTPA Ester of the 2,3-Dehydro Derivative of Hoiamide B (6): pale yellow, amorphous solid; ^{1}H NMR ($CDCl_3$, 600 MHz) δ_H 8.70 (1H, br s, NH-2), 7.79 (1H, s, H-30), 6.90 (1H, q, J = 7.1 Hz, H-3), 6.77 (1H, d, J = 10.1 Hz, NH-14), 5.09 (1H, d, J = 4.1 Hz, H-6), 4.96 (1H, d, J = 9.3 Hz, H-37), 4.79 (1H, d, J = 10.2 Hz, H-35), 3.97 (1H, dd, J = 8.2, 8.0 Hz, H-13), 3.86 (1H, br s, OH-13), 3.82 (1H, d, J = 11.6 Hz, H-22a), 3.79 (1H, d, J = 10.5 Hz, H-33), 3.74 (1H, dd, J = 9.5, 8.7 Hz, H-14), 3.69 (1H, d, J = 11.4 Hz, H-26a), 3.32 (1H, d, J = 11.4 Hz, H-26b), 3.25 (1H, d, J = 11.6 Hz, H-22b), 3.17 (3H, s, H-45), 2.78 (1H, d, J = 15.4 Hz, H-32a), 2.70 (1H, dd, J = 15.3, 10.2 Hz, H-32b), 2.48 (1H, dq, J = 7.1, 7.1 Hz, H-12), 2.32 (1H, ddq, J = 10.4, 3.7, 6.9 Hz, H-34), 2.11 (1H, m, H-7), 2.08 (1H, m, H-36), 1.84 (3H, s, H-27), 1.76 (3H, d, J = 7.1 Hz, H-4), 1.74 (1H, m, H-38), 1.68 (1H, m, H-8a), 1.55 (3H, s, H-23), 1.44 (1H, m, H-15), 1.40 (1H, m, H-16a), 1.31 (3H, d, J = 7.1 Hz, H-19), 1.30 (2H, m, H-39), 1.30 (2H, m, H-40), 1.26 (1H, m, H-8b), 1.07 (1H, m, H-16b), 1.02 (3H, d, J = 6.9 Hz, H-10), 0.97 (3H, d, J = 7.1 Hz, H-43), 0.89 (3H, t, J = 7.2 Hz, H-9), 0.88 (3H, d, J = 6.9 Hz, H-18), 0.85 (3H, t, J = 7.1 Hz, H-41), 0.82 (3H, d, J = 6.8 Hz, H-42), 0.77 (3H, t, J = 7.4 Hz, H-17), 0.72 (3H, d, J = 6.9 Hz, H-44); LRESIMS m/z 1138.57 $[M + H]^+$, 1160.58 $[M + Na]^+$.

37-*R*-MTPA Ester of the 2,3-Dehydro Derivative of Hoiamide B (7): pale yellow, amorphous solid; ^{1}H NMR ($CDCl_3$, 600 MHz) δ_H 8.72 (1H, br s, NH-2), 7.78 (1H, s, H-30), 6.86 (1H, q, J = 7.0 Hz, H-3), 6.79 (1H, d, J = 10.2 Hz, NH-14), 5.08 (1H, d, J = 4.1 Hz, H-6), 4.95 (1H, dd, J = 9.6, 2.0 Hz, H-37), 4.75 (1H, d, J = 10.4 Hz, H-35), 3.96 (1H, dd, J = 7.7, 7.7 Hz, H-13), 3.92 (1H, br s, OH-13), 3.83 (1H, d, J = 11.6 Hz, H-22a), 3.77 (1H, d, J = 10.1 Hz, H-33), 3.75 (1H, dd, J = 9.5, 8.7 Hz, H-14), 3.68 (1H, d, J = 11.3 Hz, H-26a), 3.33 (1H, d, J = 11.4 Hz, H-26b), 3.24 (1H, d, J = 11.6 Hz, H-22b), 3.17 (3H, s, H-45), 2.78 (1H, d, J = 15.2 Hz, H-32a), 2.68 (1H, dd, J = 15.4, 10.3 Hz, H-32b), 2.48 (1H, dq, J = 7.1, 7.1 Hz, H-12), 2.30 (1H, ddq, J = 10.5, 3.7, 6.9 Hz, H-34), 2.11 (1H, m, H-7), 2.08 (1H, m, H-36), 1.83 (3H, s, H-27), 1.77 (1H, m, H-38), 1.75 (3H, d, J = 7.1 Hz, H-4), 1.68 (1H, m, H-8a), 1.55 (3H, s, H-23), 1.49 (1H, m, H-15), 1.43 (1H, m, H-16a), 1.32 (2H, m, H-39), 1.30 (2H, m, H-40), 1.30 (3H, d, J = 7.1 Hz, H-19), 1.25 (1H, m, H-8b), 1.08 (1H, m, H-16b), 1.02 (3H, d, J = 6.9 Hz, H-10), 0.94 (3H, d, J = 7.1 Hz, H-43), 0.92 (3H, d, J = 6.6 Hz, H-18), 0.91 (3H, t, J = 7.5 Hz, H-9), 0.86 (3H, d, J = 6.9 Hz, H-42), 0.83 (3H, t, J = 7.1 Hz, H-41), 0.80 (3H, t, J = 7.4 Hz, H-17), 0.71 (3H, d, J = 6.9 Hz, H-44); LRESIMS m/z 1138.56 $[M + H]^+$, 1160.47 $[M + Na]^+$.

Isolation of Hoiamide C (3). The cyanobacterial filaments (approximately 81 g, dry wt) were extracted repeatedly with CH_2Cl_2−MeOH (2:1) to afford 1.42 g of crude extract. A portion of the extract (1.19 g) was fractionated by silica gel VLC with a stepped gradient elution of hexanes, EtOAc, and MeOH. The bioactive fraction F (79.2 mg) was subjected to RP HPLC (Phenomenex Jupiter 10 μm C_{18}, 10 × 250 mm, 65% MeCN−H_2O at 3 mL/min, detection at 228, 254, and 280 nm) to yield 2.9 mg of hoiamide C (**3**).

Hoiamide C (3): colorless oil; $[\alpha]^{23}_D$ +16 (*c* 0.2, $CHCl_3$); CD λ 295 nm ($\Delta\varepsilon$ −0.21), λ 280 nm ($\Delta\varepsilon$ −0.11), λ 245 nm ($\Delta\varepsilon$ −0.37), λ 220 nm ($\Delta\varepsilon$ +2.42); UV (MeCN) λ_{max} 249 nm (log ε 3.66); IR (neat) ν_{max} 3389, 2925, 2853, 1731, 1656, 1520, 1182, 1084, 735 cm^{-1}; ^{1}H and ^{13}C NMR data, see Table 2; HREIMS m/z $[M]^+$ 770.3743 (calcd for $C_{37}H_{62}N_4O_7S_3$, 770.3775).

Preparation of Hoiamide C (3) from Hoiamide A (1). Hoiamide A (10.1 mg, 0.011 mmol) was dissolved in a mixture of dioxane−H_2O 2:1 (3 mL) and treated with LiOH monohydrate (10.0 mg, 0.21 mmol) at 25 °C. The mixture was stirred at room temperature until TLC (70% EtOAc in hexanes) showed the absence of starting material (1 h). The solvent of mixture was then removed under reduced pressure, and the resulting residue was redissolved in EtOH (15 mL), treated with 12 N HCl (5 μL, 0.06 mmol) at 25 °C, and stirred at the same temperature until TLC showed the appearance of a new product (72 h). At this point, the crude reaction was concentrated to dryness, reconstituted in H_2O, and extracted with EtOAc (3 × 20 mL). The organic layer was dried (Na_2SO_4) and filtered, and upon solvent removal under vacuum, the resulting residue was purified via silica gel column chromatography (70% EtOAc in hexanes) to yield pure hoaimide C (**3**) (1.3 mg, 16%) as a colorless oil: $[\alpha]^{23}_D$ +32 (*c* 0.6, $CHCl_3$); CD λ 295 nm ($\Delta\varepsilon$ −0.35), λ 280 nm ($\Delta\varepsilon$ −0.15), λ 260 nm ($\Delta\varepsilon$ +0.13), 245 nm ($\Delta\varepsilon$ −0.11), λ 220 nm ($\Delta\varepsilon$ +3.98); UV (MeCN) λ_{max} 250 nm (log ε 3.84); IR (neat) ν_{max} 3366, 2963, 2927, 1731, 1655, 1516, 1179, 1083, 671 cm^{-1}; ^{1}H NMR (600 MHz, pyridine-d_5) δ 8.30 (1H, s, H-20), 7.60 (1H, d, J = 10.1 Hz, NH-4), 7.42 (1H, d, J = 3.6 Hz, OH), 5.95 (1H, s, OH), 5.38 (1H, s, OH), 4.45 (1H, d, J = 9.0 Hz, H-3), 4.43 (1H, ddd, J = 11.4, 3.8, 2.4 Hz, H-23), 4.41 (1H, dd, J = 10.8, 1.5 Hz, H-25), 4.19 (1H, d, J = 11.4 Hz, H-12a), 4.17 (1H, m, H-36a), 4.15 (1H, dd, J = 9.6, 9.6 Hz, H-4), 4.15 (1H, d, J = 11.4 Hz, H-16a), 4.13 (1H, m, H-36b), 3.93 (1H, dd, J = 6.6, 4.9 Hz, H-27), 3.54 (1H, d, J = 10.8 Hz, H-16b), 3.51 (1H, dd, J = 15.6, 1.8 Hz, H-22a), 3.35 (3H, s, H-35), 3.33 (1H, d, J = 11.4 Hz, H-12b), 3.16 (1H, dd, J = 15.0, 10.2 Hz, H-22b), 2.92 (1H, dddd, J = 9.6, 7.2, 7.2, 7.2 Hz, H-2), 2.52 (1H, m, H-24), 2.05 (1H, m, H-26), 2.04 (3H, s, H-17), 2.02 (1H, m, H-5), 1.87 (1H, quintet, J = 6.0 Hz, H-28), 1.78 (1H, m, H-6a), 1.77 (3H, s, H-13), 1.59 (1H, m, H-29a), 1.39 (1H, m, H-6b), 1.38 (2H, m, H-30), 1.37 (1H, m, H-29b), 1.34 (3H, d, J = 7.2 Hz, H-9), 1.20 (3H, d, J = 6.6 Hz, H-33), 1.15 (3H, d, J = 6.0 Hz, H-32), 1.14 (3H, t, J = 7.2 Hz, H-37), 0.97 (3H, d, J = 6.6 Hz, H-8), 0.95 (3H, d, J = 7.2 Hz, H-34), 0.93 (3H, t, J = 7.8 Hz, H-7), 0.89 (3H, t, J = 7.2 Hz, H-31); ^{13}C NMR (125 MHz, pyridine-d_5) δ 178.9 (C-14), 176.4 (C-1), 174.8 (C-10), 170.4 (C-21), 163.6 (C-18), 148.4 (C-19), 122.1 (C-20), 85.7 (C-11), 85.0 (C-15), 81.6 (C-23), 76.4 (C-27), 71.62 (C-3), 71.57 (C-25), 60.5 (C-36), 56.8 (C-35), 54.1 (C-4), 45.3 (C-2), 43.0 (C-16), 41.9 (C-12), 37.9 (C-26), 37.3 (C-24), 37.2 (C-29), 36.7 (C-5), 35.5 (C-28), 34.2 (C-22), 27.0 (C-17), 26.4 (C-13), 26.3 (C-6), 20.7 (C-30), 16.0 (C-8), 14.8 (C-31), 14.6 (C-9), 14.5 (C-37), 14.2 (C-32), 11.5 (C-7), 10.41 (C-33), 10.38 (C-34); HRESIMS m/z $[M + H]^+$ 771.3860 (calcd for $C_{37}H_{63}N_4O_7S_3$, 771.3859).

Neocortical Neuron Culture. Primary cultures of neocortical neurons were obtained from embryonic day 16 Swiss-Webster mice. Briefly, pregnant mice were euthanized by CO_2 asphyxiation, and embryos were removed under sterile conditions. Neocortices were collected, stripped of meninges, minced by trituration with a Pasteur pipet, and treated with trypsin for 25 min at 37 °C. The cells were then dissociated by two successive trituration and sedimentation steps in soybean trypsin inhibitor and DNase containing isolation buffer, centrifuged and resuspended in Eagle's minimal essential medium with Earle's salt (MEM), and supplemented with 1 mM L-glutamine, 10% fetal bovine serum, 10% horse serum, 100 IU/mL penicillin, and 0.10 mg/mL streptomycin, pH 7.4. Cells were plated onto poly-L-lysine-coated 96-well (9 mm) clear-bottomed black-well culture plates (Costar) at a density of 1.5 × 10^5 cells/well. Cells were then incubated at 37 °C in a 5% CO_2 and 95% humidity atmosphere. Cytosine arabinoside (10 μM) was added to the culture medium on day 2 after plating to prevent proliferation of nonneuronal cells. The culture media was changed on days 5 and 7 using a serum-free growth medium containing Neurobasal Medium supplemented with B-27, 100 IU/mL penicillin, 0.10 mg/mL streptomycin, and 0.2 mM L-glutamine. Neocortical cultures were used in experiments between 8 and 13 days *in vitro* (DIV). All animal use protocols were approved by the Institutional Animal Care and Use Committee (IACUC) at Creighton University.

Intracellular Ca^{2+} Monitoring. Neocortical neurons grown in 96-well plates were used for $[Ca^{2+}]_i$ measurements at 12−13 DIV. Briefly, the growth medium was removed and replaced with dye loading buffer (50 μL/well) containing 4 μM fluo-3 and 0.04% pluronic acid F-127 in Locke's buffer (8.6 mM Hepes, 5.6 mM KCl, 154 mM NaCl, 5.6 mM glucose, 1.0 mM $MgCl_2$, 2.3 mM $CaCl_2$, 0.0001 mM glycine, pH 7.4). After 1 h incubation in dye loading buffer, the neurons were washed four times in fresh Locke's buffer (200 μL/well) using an automated cell washer (BioTek instrument, Inc., Winooski, VT) and transferred to a FlexStation II (Molecular Devices, Sunnyvale, CA). The final volume of Locke's buffer in each well was 150 μL. Cells were excited at 485 nm, and Ca^{2+}-bound Fluo-3 emission was detected at 535 nm. Fluorescence readings were taken once every 1.5 s for 60 s to establish the baseline, and then 50 μL of hoiamide analogue solution (4×) was added to each well from the compound plate at the rate of 52 μL/s, yielding a final volume of 200 μL/well.

Intracellular Sodium Concentration ($[Na^+]_i$) Measurement. The neocortical neurons cultured in 96-well plates (DIV 8−13) were washed four times with Locke's solution using an automated cell washer (Bioteck Instrument Inc.). The background fluorescence of each well was measured and averaged prior to dye loading. Cells were then incubated for 1 h at 37 °C with dye loading buffer (50 μL/well) containing 10 μM SBFI-AM and 0.02% Pluronic F-127. After 1 h incubation in dye loading medium, cells were washed five times with Locke's buffer, leaving a final volume of 150 μL in each well. The plate was then transferred to the plate chamber of a FlexStation II

(Molecular Devices, Sunnyvale, CA). Cells were excited at 340 and 380 nm, and Na^+-bound SBFI emission was detected at 505 nm. Fluorescence readings were taken once every 5 s for 60 s to establish the baseline, and then 50 μL of hoiamide analogue containing solution (4×) was added to each well from the compound plate at a rate of 52 μL/s, yielding a final volume of 200 μL/well.

Data Analysis. Time−response and concentration−response graphs were generated using Graphpad Prism software (Graphpad Software Inc., San Diego, CA). The EC_{50} values were determined by nonlinear regression analysis using a logistic equation.

Acknowledgment. We thank A. C. Jones and T. L. Simmons for assistance with collection of the different hoiamide-producing cyanobacterial samples from Papua New Guinea, as well as A. Jansma for assistance with the Bruker 600 MHz TCI cryoprobe spectrometer (supported in part by the Skaggs School of Pharmacy and Pharmaceutical Sciences, UCSD). Support of chemical and pharmacological aspects of the work was provided by NIH NS053398. We further acknowledge the NSF CHE-0741968 for support of the JEOL and ^{13}C-sensitive Varian NMR spectrometers in the Department of Chemistry and Biochemistry, UCSD.

Supporting Information Available: LR- and HRESIMS, one-dimensional (^1H and ^{13}C) and two-dimensional (COSY, TOCSY, HSQC, HMBC, ROESY, HETLOC, and HSQMBC) NMR spectra of **2**, **3**, **6**, and **7**, LC-ESIMS profile and CD spectra of natural and semisynthetic **3**, and bioassay results of **1** and **2**. This material is available free of charge via the Internet at http://pubs.acs.org.

References and Notes

(1) Tidgewell, K.; Clark, B. T.; Gerwick, W. H. In *Comprehensive Natural Products Chemistry*, 2nd ed.; Moore, B.; Crews, P., Eds.; Elsevier: Oxford, UK, 2010; pp 141−188.

(2) (a) Fitch, C. P.; Bishop, L. M.; Boyd, W. L.; Gortner, R. A.; Rogers, C. F.; Tilden, J. E. *Cornell Vet.* **1934**, *24*, 30–39. (b) Walsh, P.; Fleming, L.; Solo-Gabriele, H.; Gerwick, W. H., Eds. *Oceans and Human Health, Risks and Remedies from the Sea*; Elsevier Press: Oxford, UK, 2008.

(3) Marner, F.-J.; Moore, R. E.; Hirotsu, K.; Clardy, J. *J. Org. Chem.* **1977**, *42*, 2815–2819.

(4) (a) Gerwick, W. H.; Proteau, P. J.; Nagle, D. G.; Hamel, E.; Blokhin, A.; Slate, D. *J. Org. Chem.* **1994**, *59*, 1243–1245. (b) Blokhin, A. V.; Yoo, H. D.; Geralds, R. S.; Nagle, D. G.; Gerwick, W. H.; Hamel, E. *Mol. Pharmacol.* **1995**, *48*, 523–531. (c) Marquez, B. L.; Watts, K. S.; Yokochi, A.; Roberts, M. A.; Verdier-Pinard, P.; Jimenez, J. I.; Hamel, E.; Scheuer, P. J.; Gerwick, W. H. *J. Nat. Prod.* **2002**, *65*, 866–871. (d) Wu, M.; Okino, T.; Nogle, L. M.; Marquez, B. L.; Williamson, R. T.; Sitachitta, N.; Berman, F. W.; Murray, T. F.; McGough, K.; Jacobs, R.; Colsen, K.; Asano, T.; Yokokawa, F.; Shioiri, T.; Gerwick, W. H. *J. Am. Chem. Soc.* **2000**, *122*, 12041–12042. (e) Orjala, J.; Nagle, D. G.; Hsu, V.; Gerwick, W. H. *J. Am. Chem. Soc.* **1995**, *117*, 8281–8282. (f) Luesch, H.; Yoshida, W. Y.; Moore, R. E.; Paul, V. J.; Corbett, T. H. *J. Am. Chem. Soc.* **2001**, *123*, 5418–5423. (g) Luesch, H.; Chanda, S. K.; Raya, R. M.; DeJesus, P. D.; Orth, A. P.; Walker, J. R.; Izpisúa Belmonte, J. C.; Schultz, P. G. *Nat. Chem. Biol.* **2006**, *2*, 158–167.

(5) Jones, A. C.; Gu, L.; Sorrels, C. M.; Sherman, D. H.; Gerwick, W. H. *Curr. Opin. Chem. Biol.* **2009**, *13*, 216–223.

(6) Clare, J. J.; Tate, S. N.; Nobbs, M.; Romanos, M. A. *Drug Discovery Today* **2000**, *5*, 506–520.

(7) (a) Catterall, W. A.; Cestele, S.; Yarov-Yarovoy, V.; Yu, F. H.; Konoki, K.; Scheuer, T. *Toxicon* **2007**, *49*, 124–141. (b) Denac, H.; Mevissen, M.; Scholtysik, G. *Naunyn-Schmiedebergs Arch. Pharmacol.* **2000**, *362*, 453–479. (c) Taylor, C. P.; Meldrum, B. S. *Trends Pharmacol. Sci.* **1995**, *16*, 309–316. (d) Cestele, S.; Catterall, W. A. *Biochimie* **2000**, *82*, 883–892.

(8) (a) Pereira, A.; Cao, Z.; Murray, T. F.; Gerwick, W. H. *Chem. Biol.* **2009**, *16*, 893–906. (b) Pereira, A.; Cao, Z.; Murray, T. F.; Gerwick, W. H. *Chem. Biol.* **2009**, *16*, 1208.

(9) Mamer, O. A. *Methods Enzymol.* **2000**, *324*, 3–10.

(10) Grindberg, R. V.; Shuman, C. F.; Sorrels, C. M.; Wingerd, J.; Gerwick, W. H. In *Modern Alkaloids, Structure, Isolation, Synthesis and Biology*; Fattorusso, E., Taglialatela-Scafati, O., Eds.; Wiley-VCH Verlang GmbH: Weinheim, Germany, 2008; pp 139−170.

(11) Namikoshi, M.; Murakami, T.; Fujiwara, T.; Nagai, H.; Niki, T.; Harigaya, E.; Watanabe, M. F.; Oda, T.; Yamada, J.; Tsujimura, S. *Chem. Res. Toxicol.* **2004**, *17*, 1692–1696.

(12) Ramaswamy, A. V.; Sorrels, C. M.; Gerwick, W. H. *J. Nat. Prod.* **2007**, *70*, 1977–1986.

(13) Dravid, S. M.; Baden, D. G.; Murray, T. F. *J. Neurochem.* **2004**, *89*, 739–749.

(14) Dravid, S. M.; Murray, T. F. *Brain Res.* **2004**, *1006*, 8–17.

(15) Komárek, J.; Anagnostidis, K. In *Süßwasserflora von Mitteleuropa*; Büdel, B.; Gärtner, G.; Krienitz, L.; Schagerl, M., Eds.; Gustav Fischer: Jena, 2005; *19/2*, pp 483−606.

(16) Edgar, R. C. *BMC Bioinf.* **2004**, *32*, 1792–1797.

(17) Cannone, J. J.; Subramanin, S.; Schnare, M. N.; Collett, J. R.; D'Souza, L. M.; Du, Y.; Feng, B.; Lin, N.; Madabusi, L. V.; Muller, K. M.; Pnde, N.; Schang, Z.; Yu, N.; Gutell, R. R. *BMC Bioinf.* **2002**, *3*, 1471–2105.

(18) Posada, D.; Crandall, K. A. *Bioinformatics* **1998**, *14*, 817–818.

(19) Guindon, S.; Gascuel, O. *Syst. Biol.* **2003**, *52*, 696–704.

(20) Ronquist, F.; Huelsenbeck, J. P. *Bioinformatics* **2003**, *12*, 1572–1574.

(21) Nylander, J. A. A.; Wilgenbusch, J. C.; Warren, D. L.; Swofford, D. L. *Bioinformatics* **2008**, *15*, 581–583.

(22) Fujii, K.; Ikai, Y.; Oka, H.; Suzuki, M.; Harada, K. *Anal. Chem.* **1997**, *69*, 5146–5151.

(23) Pattenden, G.; Thom, S. M.; Jones, M. F. *Tetrahedron* **1993**, *49*, 2131–2138.

NP100468N